metals

MDPI

Article

Effects of Welding Parameters on Strength and Corrosion Behavior of Dissimilar Galvanized Q&P and TRIP Spot Welds

Pasquale Russo Spena [1,*], Stefano Rossi [2] and Rudi Wurzer [1,2]

[1] Faculty of Science and Technology, Free University of Bozen-Bolzano, Piazza Università 5, 39100 Bolzano, Italy; rudi.wurzer@hotmail.com

[2] Department of Industrial Engineering, University of Trento, Via Sommarive 9, 38123 Trento, Italy; stefano.rossi@unitn.it

* Correspondence: pasquale.russospena@unibz.it; Tel.: +39-0471-017-112

Received: 7 November 2017; Accepted: 24 November 2017; Published: 1 December 2017

Abstract: This study investigates the effects of the main welding parameters on mechanical strength and corrosion behavior of galvanized quenching and partitioning and transformation induced plasticity spot welds, which are proposed to assemble advanced structural car elements for the automotive industry. Steel sheets have been welded with different current, clamping force, and welding time settings. The quality of the spot welds has been assessed through lap-shear and salt spray corrosion tests, also evaluating the effects of metal expulsion on strength and corrosion resistance of the joints. An energy dispersive spectrometry elemental mapping has been used to assess the damage of the galvanized zinc coating and the nature of the corrosive products. Welding current and time have the strongest influence on the shear strength of the spot welds, whereas clamping force is of minor importance. However, clamping force has the primary effect on avoiding expulsion of molten metal from the nugget during the joining process. Furthermore, clamping force has a beneficial influence on the corrosion resistance because it mainly hinders the permeation of the corrosive environment towards the spot welds. Although the welded samples can exhibit high shear strength also when a metal expulsion occurs, this phenomenon should be avoided because it enhances the damage and vaporization of the protective zinc coating.

Keywords: resistance spot welding; advanced high strength steel; galvanized steel; welding parameters; mechanical strength; metal expulsion; corrosion behavior

1. Introduction

Automotive industries are continuously reducing the weight of vehicles to limit gas emissions and fuel consumption, maintaining or improving crashworthiness and passenger comfort. To meet all of these requirements, advanced high strength steels (AHSS) are increasingly employed in the fabrication of structural car body components and new AHSS grades are under research and development to improve their strength and toughness. In this regard, quenching and partition (Q&P) steels represent one of the most promising steel grades that are devoted to the fabrication of lightweight automotive components [1,2]. They have an austenitic-martensitic microstructure that allows for obtaining remarkable mechanical performances: the mechanical strength and elongation at fracture of Q&P steels normally range from 800 to 1200 MPa, and from 10% to 25%, respectively [1–4].

Resistance spot welding (RSW) is the most widespread technology to join structural car parts [5,6]. The main advantages of RSW are precision, the possibility to automatize the welding process, and the high joining speed. Since spot welds are discontinuity points in a car structural framework, and directly involved in transmitting loads in case of a crash event, their integrity and mechanical performances

are of the utmost importance to ensure an adequate passenger safety. Moreover, harshness, noise, and vibrations of a car can be affected by an improper quality of spot welds. Corrosion phenomena can boost these negative issues because they reduce significantly spot weld strength and its capability to absorb energy during a vehicle accident. In this regard, corrosion can remove some metal from spot welds and/or cause the formation of cracks, thus reducing the cross sectional area sustaining external loads. When considering the limited size of spot joints, this aspect must be considered with careful attention.

Currently, Q&P steels have not applications in the automotive industry, if not for some prototypes, and few works about welding of this steel grade are in the literature. Wang et al. [7] found that there are no significant differences between mechanical strength of Q&P spot welds and those obtained with dual phase steel sheets with a similar tensile strength (1000 MPa) and thickness (1.6 mm). Dissimilar welding of Q&P sheets was investigated by Russo Spena et al., evaluating the effects of the main welding parameters on the mechanical properties of spot welds that were obtained with twinning induced plasticity (TWIP) steels [8] and transformation induced plasticity (TRIP) steels [9], which were welded with similar conditions. They noted that Q&P dissimilar welded joints could reach notable lap shear strength values with proper welding conditions. However, metal expulsion limited the maximum achievable strength in Q&P/TWIP joints (17 kN vs. 22 kN of Q&P/TRIP joints) because of the lower heat conductivity and melting point of TWIP steel.

Overall, corrosion is one of the most important factors that limit vehicle lifetime, especially when different materials are welded together as dissimilar joints, because of the possible occurrence of galvanic corrosion [10–12]. Consequently, automotive companies have always adopted different techniques to protect car components from environmental corrosion [13]. In this regard, hot dip galvanization is the most common way to preserve steel sheet parts, such as door panels, pillars, rails, and so forth, from environmental corrosion. The thickness of zinc coating normally ranges from 7 to 20 μm.

During a RSW process of Zn-galvanized steels, the superficial layer can completely vaporize, and only residual Zn traces can be present on the sheet surfaces close to the spot weld after its solidification [14,15]. The partial or full removal of zinc generally favors the formation of galvanic couplings: the surrounding zinc acts as an anodic area with increasing of the corrosion rate. In addition, the formation of crevices favors different oxygen diffusion conditions, with a localization of the corrosion attack. The modification of the original microstructures in the heat affected zone could be another critical point for the corrosion behavior of spot welds [16]. The assessment of the corrosion behavior of welded joints is further complicated by their complex morphology and chemical composition. In fact, the presence of the joint represents a discontinuity of the sheets, where flat surfaces are replaced by a region with an irregular geometry, roughness, and chemical composition, which have significant effects on the overall corrosion resistance. These features are particularly critical when sheets that are made of different materials are welded together, protective coatings are damaged by the joining process, and metal expulsions and splashes occur.

The most used electrochemical corrosion measurements, in direct and alternate currents, supply results that are averaged over the all analyzed area [17]. In fact, they are not able to discern the single contributions of the sheets and of the joint to the corrosion resistance. Therefore, corrosion data are dependent on the extent of the area examined. For these reasons, it should be necessary to separate the welded parts or to isolate the joint cross section before carrying out the electrochemical tests [17–20], or to use a particular testing geometry to confine the welding area [21]. Overall, studies have pointed out that the localization of corrosion attack in the weaker zones influences the global corrosion resistance of welded joints [19,22]. Localized electrochemical techniques, such as Scanning Kelvin Probe (SKP) and Scanning Vibrating Electrode Technique (SVET), could be a possible alternative to examine joint corrosion behavior in detail [17,23–25]. Nevertheless, these techniques need of flat surfaces with a controlled low roughness, which cannot be obtained for a welded joint. Moreover, these tests only give information about a local corrosion behavior, which usually differs from the global behavior of joints. For these reasons, simpler corrosion tests, such as immersion test in aggressive

solution [26] or atmosphere (as salt spray test) [10,11] are in several cases more representative of the actual joint corrosion behavior. Among these tests, salt spray exposure is the most common and important corrosion test that is employed in the automotive industry. It allows assessing the corrosion progression on metal parts by evaluating their surface appearance after different time intervals. However, the only optical observation of the external surfaces of spot welded components normally does not allow for obtaining a complete characterization. The possible presence of crevice corrosion and galvanic corrosion phenomena, which are the typical corrosion phenomena of welded galvanized steels [10,12], on the internal surfaces close to the spot weld can be only assessed by mechanically separating the two welded sheets, and analyzing the corrosion products using a scanning electron microscope and elemental mapping [27]. Welding parameters can influence the corrosion resistance of spot welds because they drive the joint size and shape, as well as the amount of zinc coating that vaporizes during the joining process and its damage. Furthermore, improper welding settings can cause metal expulsion and the formation of metal splashes around the joints, at the interface of the two sheets, which damage further the zinc coating [16]. Overall, the literature studies have mainly focused on the corrosion resistance of Zn-galvanized sheets as a whole, often without referring to the corrosion behavior of their joints. Moreover, there is a lack of information about the damage of the zinc coating near the spot welds in the region between the two overlapped sheets, and the effect that metal expulsion has on it.

An understanding of the influence of welding parameters on the mechanical strength and corrosion resistance of dissimilar spot welds of Q&P and other steel grades is essential in driving the possible employment of Q&P steels in the transport industry, as well as to guarantee basic requirements in terms of safety and reliability of the car structure. Since TRIP steels are one of the most common AHSS grades that are employed in the automotive industry (e.g., pillar reinforcements, cross members, bumper reinforcements, sills), this work aims at evaluating the effects of the main welding parameters on the integrity and mechanical performances of Q&P/TRIP spot welds, as well as on their corrosion behavior. To this purpose, Q&P and TRIP sheets were welded using different levels of current, clamping force, and welding time and were then subjected to lap shear tests to assess spot weld strength. A salt spray exposure test was carried out to assess the corrosion behavior of the spot welds. The morphology of the corroded spot welds and the nature of the corrosion products have also been determined through SEM (scanning electron microscopy) and energy dispersive spectrometry (EDS), respectively. The joint corrosion resistance has been evaluated as a function of the welding parameters.

2. Materials and Methods

Industrial hot dip galvanized Q&P and TRIP (grade 800) steel sheets (10 ± 1 µm zinc thickness), with a thickness of 1.1 mm and 1.5 mm, respectively, have been selected for this work. The chemical compositions of Q&P and TRIP steels are reported in Table 1, whereas Table 2 lists their main mechanical properties.

Table 1. Chemical composition (wt %) of quenching and partition (Q&P) and transformation induced plasticity (TRIP) steels, as measured by optical emission spectroscopy.

Steel	% C	% Mn	% Si	% P + S	% Al	% Ti	% Nb	% Fe
Q&P	0.22	1.88	1.41	<0.02	0.04	-	<0.001	Bal.
TRIP	0.20	2.23	0.31	<0.02	1.05	0.01	0.022	Bal.

Table 2. Main mechanical properties of Q&P and TRIP steels. HV30: Vickers hardness; YS: yield strength; UTS: ultimate tensile strength; e_f: elongation at fracture; n: strengthening exponent.

Steel	Hardness (HV30)	YS (MPa)	UTS (MPa)	e_f (%)	n
Q&P	260	655	1000	22	0.10
TRIP	225	525	890	27	0.20

TRIP and Q&P sheets were cut from large sheets into 105 mm × 45 mm and 40 mm × 40 mm coupons. The larger coupons were welded in a lap-joint configuration at the center of the 35 mm overlapped position, as shown in Figure 1a, and were subjected to shear tests. The smaller coupons were completely overlapped and spot welded at the center, as displayed in Figure 1b. This last geometry was employed in the accelerated corrosion test (salt spray test) to simulate the actual service life of a spot joint.

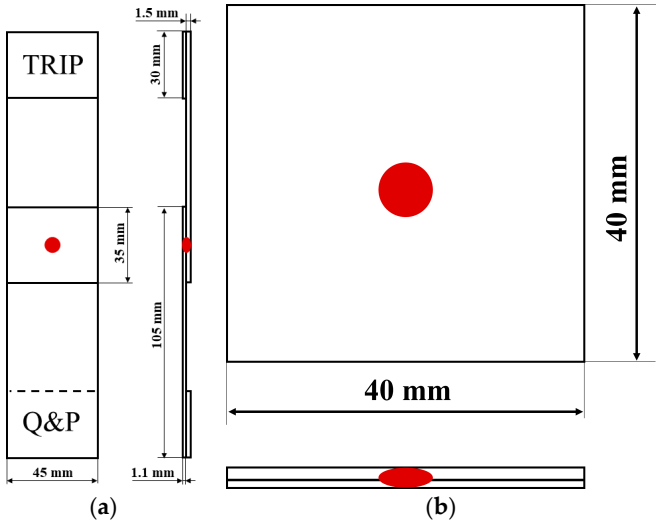

Figure 1. Size of the (**a**) lap shear and (**b**) salt spray specimens. The red spot represents the spot weld in the welded samples. Drawings not to scale.

The two types of coupons were joined using four different settings of welding parameters, as illustrated in Table 3. These settings were defined based on the previous study of Russo Spena et al. [9] about the weldability of Q&P and TRIP steels. Basically, the minimum welding current was chosen to obtain a complete button pull fracture of the spot welds during a manual peel test (a convenient and easy way to roughly assess the quality of a spot weld), whereas the maximum current was set when metal expulsions occurred. In this way, it has been possible to cover a proper range of welding settings with the experimental tests. RSW experiments were conducted with a spot welding machine with a medium frequency current of 1 kHz, and were equipped with two water cooled Cu-Cr electrodes with a tip diameter of 6 mm.

Table 3. Settings of the joining parameters employed in the welding tests.

Run No.	Current (kA)	Clamping Force (kN)	Welding Time (ms)
1	6	2	200
2	7.5	3	450
3	7.5	4	200
4	9	2	450

The occurrence of metal expulsions was assessed by measuring in real-time the voltage between the electrode tips and the welding current through the sheet stack during the welding process. From these data, the electrical resistance of the sheet stack (dynamic resistance) and the thermal input developed by the Joule effect, calculated as the integral over time of the electrical power developed, were also computed during the joining process. These parameters allow to accurately identify the occurrence of a single or multiple metal expulsions during the welding process, and to try to find a correlation between expulsions and the corrosion behavior of spot welds. Electrode voltage was measured with electrical wires directly clipped on the electrode tips. Welding current was measured

with a toroidal electrical transducer (Rogowski coil; CIE s.r.l, Grugliasco, Italy). An analog-to-digital converter with a rate of 100 kHz per channel and 16 bit resolution NI USB-6211 (National Instruments, Austin, TX, USA) was employed for the data acquisition. More details about the monitoring of a resistance spot welding process can be found in [5,9].

The lap shear tests were conducted based on the AWS D8.9M standard [28], using an electromechanical universal testing machine MTS mod. Criterion 42 (MTS Systems Corporation; Eden Prairie, MN, USA). Shear strength was defined as the peak load reached during the test. The ability of the spot welds to absorb energy during plastic deformation was defined as the area under the load-displacement curve calculated up to the peak load (i.e., the work done when the welded specimen is stressed up to the peak load).

Further sheet specimens were also welded in accordance with Table 3 and were subjected to a microstructural examination to determine the nugget size using an optical microscope Optika mod. IM-3MET (Optika, Ponteranica, Italy).

The corrosion behavior of the welded specimens has been determined by means of a salt spray exposure test conducted for 500 h, according to the ISO 9227 standard (5 wt % NaCl solution and 40 °C of chamber temperature) [29]. The salt spray machine was an Erichsen mod. 610/400E (Erichsen GmbH & Co., Hemer, Germany). Samples were positioned at an angle of 20°, with respect to the vertical axis. Following the standard recommendations, a visual inspection of exposed samples was carried out to monitor the damage level at 24 h, 48 h, 168 h, and 500 h (the end of the test). At end of exposure time, the welded joints were fractured manually, separating the two sheets, in order to evaluate the state of corrosion on the internal surfaces surrounding the Q&P/TRIP joints. The appearance of the corroded joints has been evaluated by means of a stereoscopic optical Nikon SMZ 25 microscope (Nikon Instruments Inc., Tokyo, Japan). The morphology of corrosion attack was observed using a JEOL T300 SEM in backscattered BSE mode (Jeol Ltd., Tokyo, Japan). The nature of the corrosion products and the distribution of Fe, Zn, O, and Cl in the corroded areas have been assessed through an EDS Bruker analyser (Bruker, Billerica, MA, USA).

3. Results and Discussion

3.1. Spot Welding and Joint Features

TRIP steel has a mixed microstructure that consists of ferrite, austenite, and bainite, as shown in Figure 2a. Q&P steel is characterised by an austenitic and martensitic microstructure, whose volume fractions are about 60% and 40%, respectively, Figure 2b.

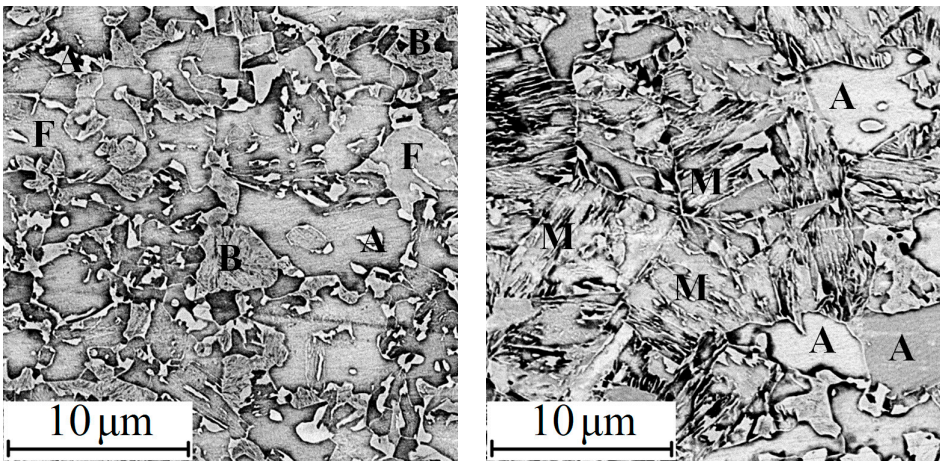

(**a**) (**b**)

Figure 2. Microstructure of (**a**) TRIP and (**b**) Q&P steels: austenite (A), bainite (B), ferrite (F), and martensite (M).

Figure 3 displays the typical electrode voltage, welding current, and dynamic resistance signals that were obtained during the spot welding of Q&P and TRIP sheets. Particularly, Figure 3a shows the signals obtained during a spot welding process without the occurrence of metal expulsion, whereas Figure 3b displays the signals that are typical of a spot welding process with metal expulsion. A metal expulsion is the result of an excessive pressure of molten material in the forming joint. As soon as some molten metal is expelled out, the liquid pressure in the nugget reduces and the containment of the surrounding solid avoids further losses of metal. However, if the excessive liquid pressure is again achieved inside the nugget, a further metal expulsion can occur. The number of these expulsions rises as the clamping force decreases because liquid metal can achieve a critical pressure several times during the joining process, and when the welding currents and times increase because more liquid metal forms. This is coherent with the occurrence of the multiple expulsions that happened in samples no. 4, Figure 3b, which were welded with the lowest clamping force and the highest welding current and time. Metal ejection normally originates local material discontinuities (i.e., voids) within the joint, thus inducing a sudden drop of the electrical resistance of the sheet stack and of the electrode voltage, while the welding current increases. The corresponding signal variations are all the more intense the higher amount of the expelled material is. Samples no. 1, 2, and 3 did not exhibit any significant metal expulsion, giving welding signals similar to those illustrated in Figure 3a. Contrarily, samples no. 4 exhibited multiple metal expulsions, as they can be detected by the abrupt changes of the signal curves displayed in Figure 3b.

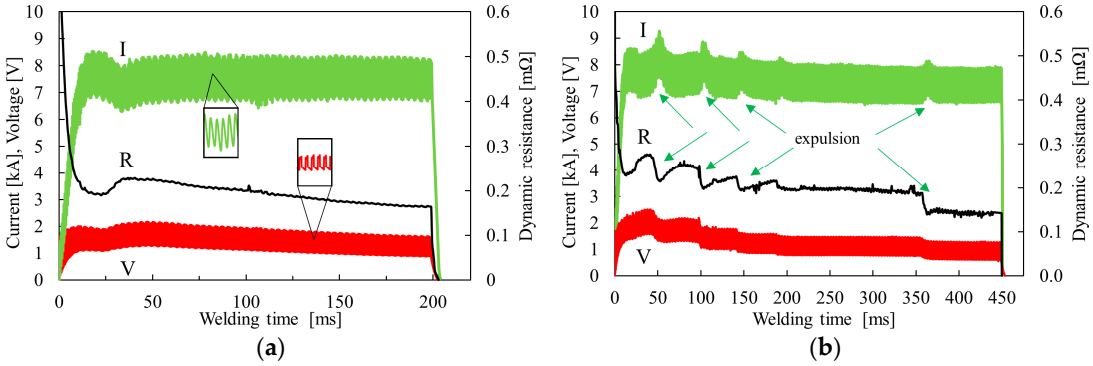

Figure 3. Welding current, electrode voltage and dynamic resistance signals as obtained from runs (**a**) no. 1 and (**b**) no. 4. I and V, real values; R, root mean square (RMS) values.

Dissimilar spot welds normally exhibit asymmetrical nuggets because of the different nature of the joined sheets, and hence of their thermal and electrical properties, and thickness [5,8,9,30]. Figure 4 shows a centered cross section of an etched Q&P/TRIP spot weld. It can be noted that the nugget at the TRIP side is bigger. Since the thermal and electrical properties of Q&P and TRIP steels should be very similar (refer to their chemical compositions in Table 1), the nugget asymmetry is mainly ascribable to their different thicknesses of the two sheets.

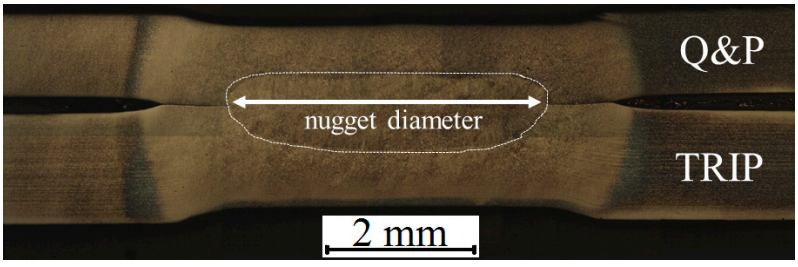

Figure 4. Typical nugget appearance through a centered cross sectional area of a Q&P/TRIP joint after chemical etching. Image from sample no. 1.

Figure 5 displays the nugget size of the spot welds at varying welding conditions. It can be pointed out that the nugget increases following this order, Figure 5a: run no. 1, 3, 4, and 2. The nugget size is directly related to the heat energy provided during the joining process. As expected, higher welding currents and longer times promote the formation of larger nuggets. Clamping force has instead an opposite effect: large clamping forces widen the contact area between the electrode tips and the sheets, thereby reducing the overall contact resistance, and, in turn, the heat that is generated by the Joule effect in the sheet stack [5]. Samples no. 1 were joined with the lowest welding current and time, thus they exhibit the smallest nuggets. Although samples no. 4 were realized with a higher welding current and a lower clamping force (which allowed to provide the largest thermal input, as shown in Figure 5), they show a nugget size similar to that of samples no. 2. This is attributed to the occurrence of metal expulsion that limits the maximum achievable nugget size.

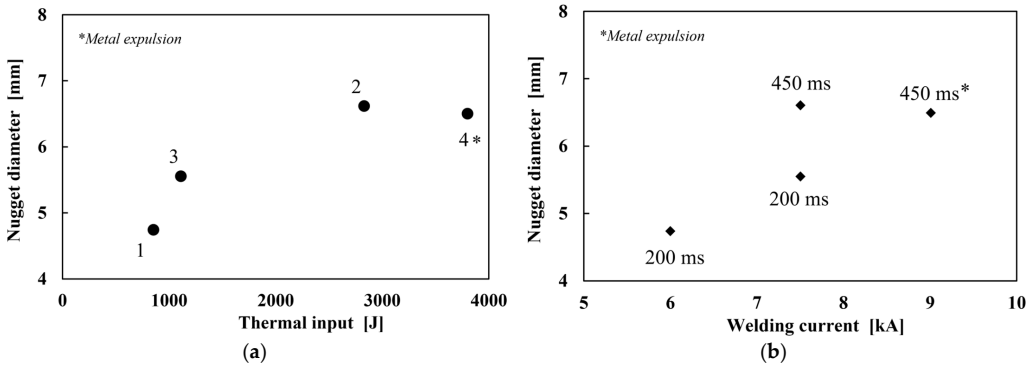

Figure 5. Average nugget diameter of the spot welds: influence of (**a**) the thermal input by Joule effect and (**b**) welding current and time for the different welding conditions.

3.2. Mechanical Properties of Spot Welds

Coherently with the literature about resistance spot welding [5,8,9,30–33], there is a clear relationship between the shear strength and the nugget size of the Q&P/TRIP spot welds. In particular, shear strength increases as nugget diameter widens, Figure 6. In this regard, samples no. 2 and 4 exhibit the higher shear strengths. When comparing the shear strength values of samples no. 1 and 3, which were joined with the same welding time, the increase of current from 6 to 7.5 kA has led to a bigger nugget size in samples no. 3 more than the reduced clamping force from 3 to 2 kN (as discussed previously, this favors the development of higher thermal inputs in the joint) did in samples no. 1. Therefore, as for the effects of the welding parameters on nugget size, it can be claimed that welding current and time have the strongest effect on spot strength, whereas the effect of clamping force is secondary.

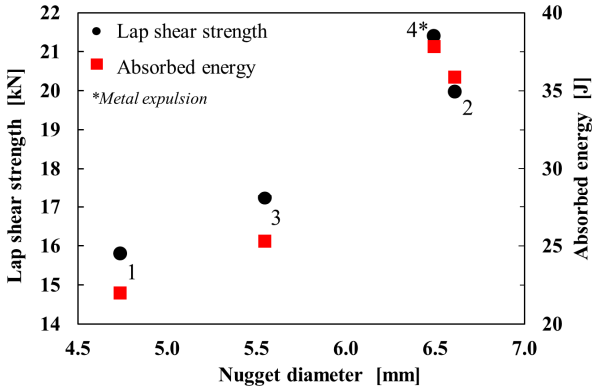

Figure 6. Average lap shear strength and absorbed energy of Q&P/TRIP spot welds for the different welding conditions.

Figure 6 also shows that even if metal expulsion occurred in sample no. 4 (refer to Figure 3b), the highest welding current and time have led to the formation of large nuggets, and, hence, to high shear strengths. Samples no. 2 exhibit a slightly larger nugget than samples no. 4, and even if they did not experience any metal expulsion, they exhibit lower strength values. This contrariety could be ascribable to the stronger electrode indentation in samples no. 2, which are caused by the higher clamping force employed, that could induce high stress concentrations in the sheets surface close to the spot [31,34]. On the other hand, it is presumable that metal expulsion has limited the maximum achievable shear strength. In addition, even though metal expulsion has had a less pronounced detrimental effect on shear strength, it generally has under tensile stresses. This is because defects within (e.g., porosities, cracks) and around the joint (e.g., metal splashes, cracks) are less sensitive to shear than tensile stress fields.

3.3. Corrosion Behavior

At first, the influence of the welding parameters on the corrosion behavior of the spot welds has been evaluated through a visual inspection of the external side of the joints during the salt spray exposure test. Regardless to the welding conditions, all of the welded samples exhibit a similar level of corrosion without any significant differences for the examined exposure times (24 h, 48 h, 168 h, and 500 h). Figure 7 shows the typical damages that occurred on the external surfaces of the spot welds. The spot weld is visible in the center of each image.

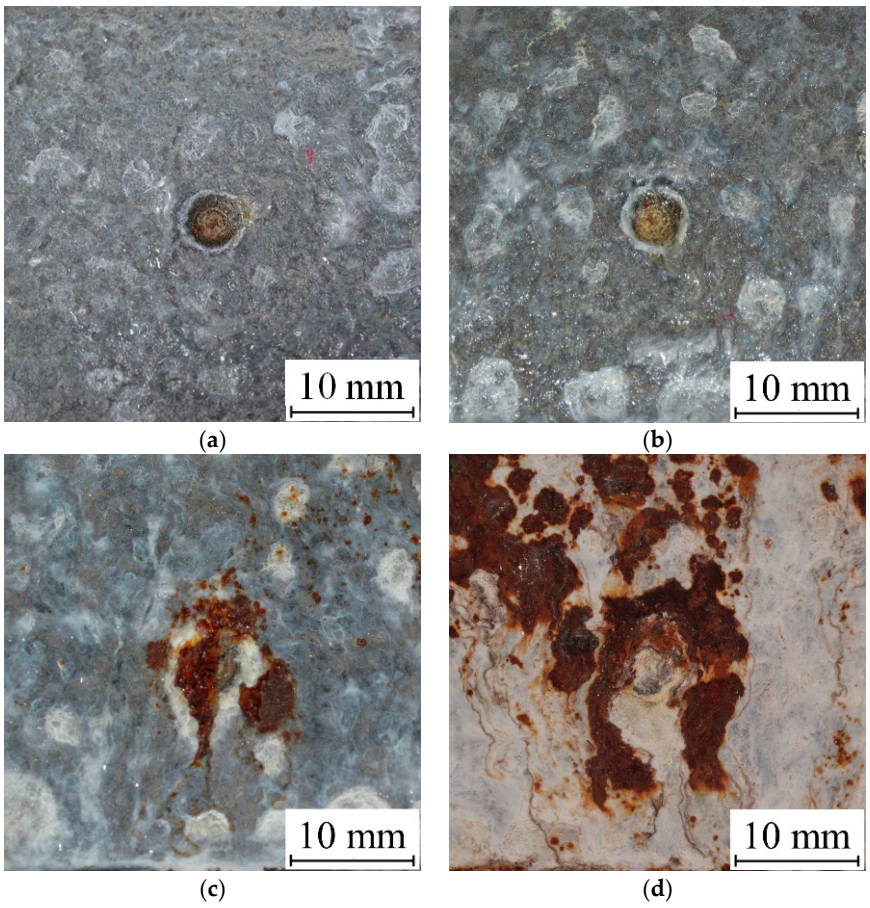

(**a**) (**b**) (**c**) (**d**)

Figure 7. State of corrosion on the external surfaces of the spot welds during the salt spray corrosion test after the following exposure times: (**a**) 24 h, (**b**) 48 h, (**c**) 168 h, and (**d**) 500 h. Images obtained from a sample welded with run no. 4.

As observed in Figure 7a, some zinc corrosion products formed on the galvanised surfaces of the steel sheets after 24 h of salt spray exposure. Due to the nature of the corrosion environment, they consist of a mixture of Zn chlorides and hydroxides with the typical white coloration. These products were almost absent on the spot weld surfaces due to a complete vaporization of the zinc layer in this region. The first signs of superficial oxidation were visible as red rust products on the spot weld surfaces and in part of the surrounding HAZ (heat affected zone). These are the regions were the zinc layer is fully or partially vaporized, therefore it was not able to preserve the steel substrate through a cathodic protection. After 48 h, Figure 7b, the amount of zinc corrosion products and superficial oxidation did not change significantly with respect to the first time interval. Steel corrosion was still mainly limited to the spot weld surface and HAZ, whereas the surrounding sheet surfaces did not show important signs of corrosion. After 168 h, the weld region was completely corroded, with the corrosion proceeding through the sheet thickness. Small corrosion spots grew in some of the zones that were adjacent to the spot weld surfaces and were then nucleated in larger areas over the time. Corrosion was unevenly distributed on the sheet surfaces far from the welded area, which were not altered by the joining process: red steel corrosion products covered some regions, whereas others only displayed a damage of the zinc layer without a corrosion of the steel substrate. This could be mainly ascribable to the intrinsic uneven distribution of the corrosive environment on sheet surfaces and to the irregular thickness of the zinc layer (it could vary from about 9 to 11 μm). At the end of the salt spray test (500 h), the entire joint surface and HAZ were completely corroded. Large regions of the sheets were also corroded significantly due to the dissolution of the zinc coating. Other regions, instead, still exhibited a residual Zn layer, which had avoided the corrosion of steel substrate.

To evaluate the corrosion damages and the corrosion morphology at the interface of the welded coupons near the spot welds, the welded samples were mechanically separated after the end of the salt spray test. The internal surfaces were examined using a SEM and elemental mapping by EDS. The visual examination of these zones also allows having an understanding about the penetration of the aggressive environment between the two sheets and close to the spot weld. Figure 8 illustrates the typical inner surfaces obtained from the spot welds at varying welding conditions.

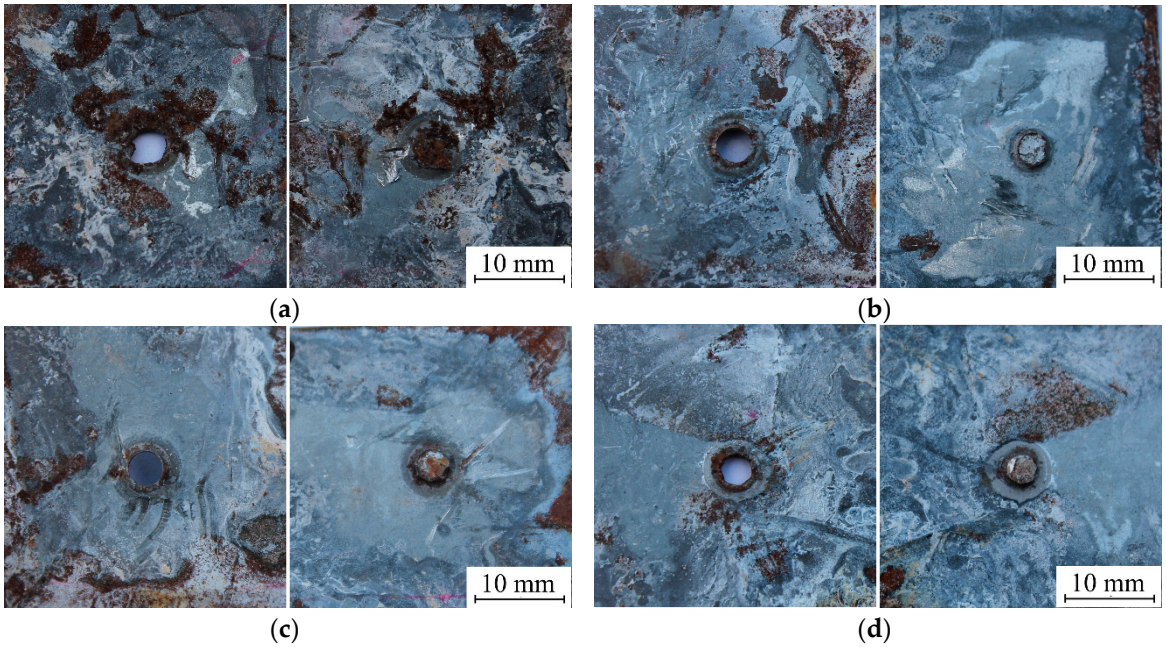

Figure 8. Surfaces of the spot welds at the internal sheet interface side after an exposure time of 500 h to a salt spray environment. Samples (**a**) no. 1; (**b**) no. 2; (**c**) no. 3; and (**d**) no. 4.

As expected, the corrosion is much more limited than that observed on the external sheet surfaces, due to the difficulty of the aggressive environment to penetrate in the space between the two sheets. Overall, coupons no. 3 are those with the best corrosion resistance, showing the most extensive areas that were still covered with a Zn layer, Figure 8c. This is because these samples were welded using the highest clamping force. In fact, a strong reduction of the space between the sheet regions near the joint prevents the permeation of the corrosive environment during the salt spray exposure. Samples no. 2, which were welded with an intermediate clamping force, display a moderate corrosion of the zinc layer around the joint, Figure 8b. Contrarily, the clamping force employed to join samples no. 1 and 4 was probably insufficient to reduce the space around the spot weld, thereby allowing for the aggressive environment to exert its corrosive action up to the spot weld, Figure 8a,d, respectively. The corrosion attack also involved the steel substrate in some regions of these samples.

Further information about the corrosion resistance of the spot welds can be obtained from an elemental mapping of the internal surfaces of the opened spot welds, by detecting Fe, Zn, O, and Cl. The presence of these chemical elements can be related to the Zn coating, Zn corrosion products (chlorides and hydroxides), iron oxidation, and to the thermal power that was developed during the joining process. Particularly, larger heat inputs and metal expulsion widen the area around the nugget where the Zn coating vaporizes or damages, thus reducing the capability of the steel substrate to resist to a corrosive attack near the spot welds. Figures 9–12 display the distribution of Fe, Zn, O, and Cl on the spot welds and their surrounding areas, as detected by the EDS mapping. Welded samples no. 1 broke by a partial thickness fracture with button pull, thus one side of the fracture samples showed a partial button pull and a fracture surface going through the nugget thickness. The borders of the head of the partial button pull and of the fracture surface located on the sheet surface are highlighted with the white bottom and top dotted lines in Figure 9, respectively. Samples no. 2, 3, and 4 broke by a full button pull. The white dotted lines in Figures 10–12 display the border of the button pull. A continuous white line is also present in each image of Figures 9–11 to point out the border of the sheet surface without the zinc layer (due to its vaporization caused by the heat input). The continuous line is not present on the images of Figure 12 because the high heat input and metal expulsion that was involved in the joining process almost removed completely the zinc coating close to the spots.

For all of the samples, Zn is nearly completely absent in the ring-shaped HAZ around the nuggets. This is due to the strong Zn vaporization that is caused by the welding current that flew through in the volume of the sheet stack that is enclosed between the two electrode tips. The extent of this region can be considered as an indirect measure of the heat that is involved in the welding process, that is, larger heat inputs widen this region. Coherently to the heat input involved in the spot welding, refer to Figure 5, the extent of the region without a zinc layer widens with the following order (Figures 9, 10, 11 and 12c): samples no. 1, 3, 2, and 4. Samples no. 2 and 3 exhibit a significant presence of Zn residuals on the surrounding areas (i.e., brighter yellow-colored areas), while lower amounts of Zn are in samples no. 1 and no. 4. As seen in Figure 8, these could be attributed to the fact that samples no. 2 and 3, although welded with different welding current and time values, were clamped with the highest clamping force. The zinc layer was severely damaged on the sheet surfaces near the spots when a metal expulsion happened, as shown in Figure 12c. The zinc coating almost disappeared and the steel substrate results became exposed. Consequently, no white rust has been found in these regions. Metal expulsion is hence dangerous for the corrosion resistance of the spot welds, since larger regions of steel are unprotected from aggressive environments. Overall, welding current and time seem to have the main effect on the damage of the Zn coating close to the weld spots, whereas clamping force primarily drives the corrosion resistance on the sheet surfaces farther from the joints.

The dark regions on the Zn-images point out where the coating layer misses. It can be noted that the distributions of Fe and Zn are complementary to each other: as Zn is absent, Fe emerges on the sheet surfaces and it can be subjected to corrosive and oxidation phenomena. The outer parts of the HAZ are characterized by a low oxides concentration, whereas their amount is considerably higher close

to the spot welds and on their surfaces. On the spot surface, oxidation can occur during the welding process due to the high temperatures that were reached in the center of the weld. The temperature decreases at increasing distance from the center of the weld, and hence a minor oxidation occurred in this intermediate ring-shaped region around the joint. At a certain distance from the spot, the adhesion between the welded sheets reduces, whereby allowing the entrance of the corrosive environment during the salt spray exposure.

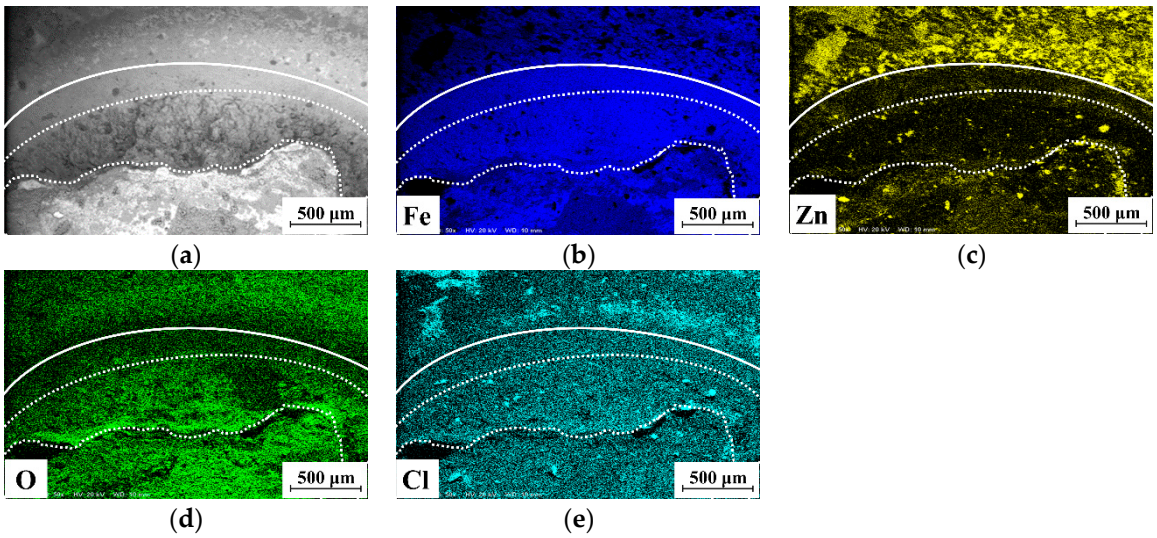

Figure 9. (**a**) SEM micrograph (BSE mode) on weld spot surface and surrounding HAZ of sample no. 1 after the salt spray exposure test. Chemical distribution of elements (**b**) Fe, (**c**) Zn, (**d**) O, and (**e**) Cl, as obtained from energy EDS analysis. White dotted lines point out the border of the fractured spot weld on the sheet (top line) and on the pull out head (bottom line). The continuous line defines the border of the sheet surface without the zinc layer.

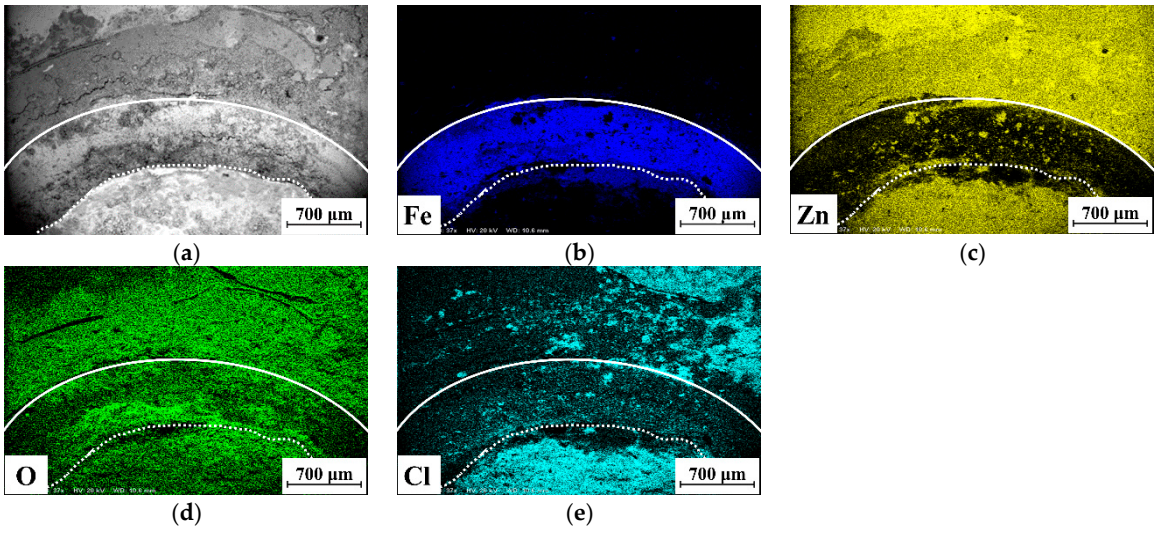

Figure 10. (**a**) SEM micrograph (BSE mode) on weld spot surface and surrounding HAZ of sample no. 2 after the salt spray exposure test. Chemical distribution of elements (**b**) Fe, (**c**) Zn, (**d**) O, and (**e**) Cl, as obtained from EDS analysis. White dotted lines point out the border of the fractured spot weld on the sheet (top line) and on the pull out head (bottom line). The continuous line defines the border of the sheet surface without the zinc layer.

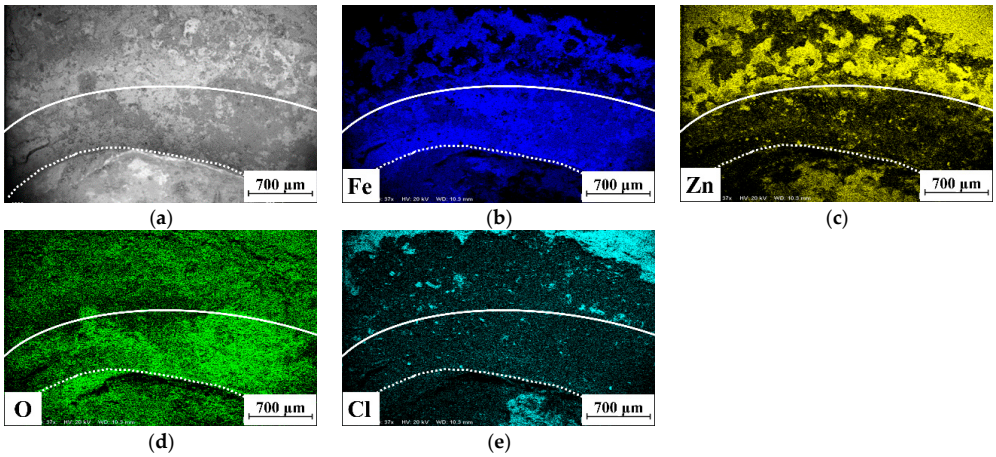

Figure 11. (**a**) SEM micrograph (BSE mode) on weld spot surface and surrounding HAZ of sample no. 3 after the salt spray exposure test. Chemical distribution of elements (**b**) Fe, (**c**) Zn, (**d**) O, and (**e**) Cl, as obtained from EDS analysis. White dotted lines point out the border of the fractured spot weld on the sheet (top line) and on the pull out head (bottom line). The continuous line defines the border of the sheet surface without the zinc layer.

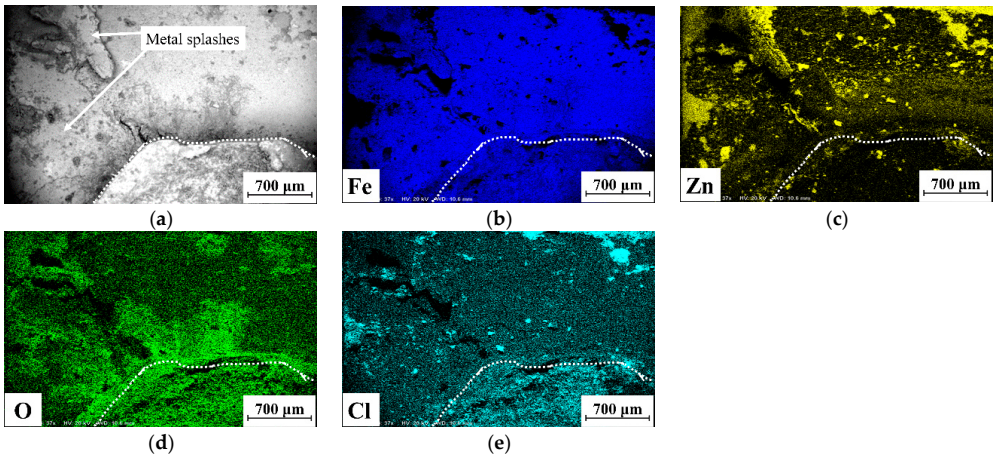

Figure 12. (**a**) SEM micrograph (BSE mode) on weld spot surface and surrounding HAZ of sample no. 4 after the salt spray exposure test. Chemical distribution of elements (**b**) Fe, (**c**) Zn, (**d**) O, and (**e**) Cl, as obtained from EDS analysis. White dotted lines point out the border of the fractured spot weld by pull out.

The presence and distribution of chlorine is a useful indicator to assess as far as corrosion environment penetrates between the sheets close to the spot weld during the salt spray chamber exposure. The elemental mapping confirms what has been found from Figure 8: the adhesion of the sheet stack, which depends mainly on the clamping force that is employed during the RSW process, limits the corrosion phenomena near the spot welds.

4. Conclusions

In this paper, the influences of the main welding parameters, namely current, clamping force, and welding time, on the mechanical strength and the corrosion behavior of dissimilar resistance spot welded galvanized Q&P and TRIP steel sheets have been investigated. SEM and elemental mapping by EDS have been used to assess the damage of the Zn coating and the nature and amount of the corrosion products near the spot welds after a salt exposure test. The effect of metal expulsion on spot strength and corrosion behavior has been determined. The main results can be summarized as follows:

(1) Welding current and time are the main factor affecting shear strength of Q&P/TRIP spot welds, clamping force has a minor influence.
(2) Clamping force has a beneficial effect on corrosion resistance of the internal side of the spot welds because it is more tightly sheltered from the corrosive environment by the surrounding sheets, being they squeezed together by the indentation of the electrode tips.
(3) The local distribution of zinc coating and corrosion products near the spot welds is highly dependent on the specific setting of the welding parameters: welding current and time seem to have the main effect on the damage of the Zn coating close to the weld spots, whereas clamping force primarily drives the corrosion resistance on the sheet surfaces farther from the joints.
(4) Metal expulsion limits that maximum achievable shear strength of the spot welds. Moreover, it leads to a stronger vaporization of the zinc coating around the spot welds, thereby exposing more steel substrate to a corrosive attack.

Overall, even though some welding conditions could lead to significant mechanical strengths of spot welds, they could not be optimal in terms of corrosion resistance. Further considerations, such as clamping force and the heat input that is developed during the joining process, should be taken into account when spot welds can be subjected to corrosive attacks during the service.

Acknowledgments: The authors thank the Department of Innovation, Research and University of the Autonomous Province of Bozen/Bolzano for covering the Open Access publication costs. Further thanks to Manuela De Maddis from Politecnico di Torino for the help with the welding tests and Gianluca D'Antonio from Politecnico di Torino for having provided the Matlab file for the elaboration of the welding data.

Author Contributions: Pasquale Russo Spena and Stefano Rossi conceived and designed the experiments; Pasquale Russo Spena performed the welding tests, Pasquale Russo Spena and Rudi Wurzer conducted the metallographic analysis, shear tests and microhardness measurements, Stefano Rossi and Rudi Wurzer performed the salt spray chamber exposure tests and corrosion characterization; all the authors have contributed to write the article.

Conflicts of Interest: The authors declare no conflict of interest.

References

1. De Moor, E.; Speer, J.G.; Matlock, D.K.; Kwak, J.H.; Lee, S.B. Effect of carbon and manganese on the quenching and partitioning response of CMnSi steels. *ISIJ Int.* **2011**, *51*, 137–144. [CrossRef]
2. Sun, J.; Yu, H. Microstructure development and mechanical properties of quenching and partitioning (Q&P) steel and an incorporation of hot-dipping galvanization during Q&P process. *Mater. Sci. Eng. A* **2013**, *586*, 100–107.
3. Yan, S.; Liu, X.; Liu, W.J.; Liang, T.; Zhang, B.; Liu, L.; Zhao, Y. Comparative study on microstructure and mechanical properties of a C-Mn-Si steel treated by quenching and partitioning (Q&P) processes after a full and intercritical austenitization. *Mater. Sci. Eng. A* **2017**, *684*, 261–269.
4. Seo, E.J.; Cho, L.; Estrin, Y.; De Cooman, B.C. Microstructure-mechanical properties relationships for quenching and partitioning (Q&P) processed steel. *Acta Mater.* **2016**, *113*, 124–139.
5. Zhang, H.; Senkara, J. *Resistance Welding: Fundamentals and Applications*, 2nd ed.; CRC Press: London, UK, 2011.
6. Akkaş, N.; Ilhan, E.; Aslanlar, S.; Varol, F. The effect of nugget sizes on mechanical properties in resistance spot welding of SPA-C atmospheric corrosion resistant steel sheets used in rail vehicles. *Mater. Test.* **2014**, *56*, 879–883. [CrossRef]
7. Wang, B.; Duan, Q.Q.; Yao, G.; Pang, J.C.; Li, X.W.; Wang, L.; Zhan, Z.F. Investigation on fatigue fracture behaviors of spot welded Q&P980 steel. *Int. J. Fract.* **2014**, *66*, 20–28.
8. Russo Spena, P.; De Maddis, M.; Lombardi, F.; Rossini, M. Dissimilar resistance spot welding of Q&P and TWIP steel sheets. *Mater. Manuf. Proc.* **2016**, *31*, 291–299.
9. Russo Spena, P.; De Maddis, M.; D'Antonio, G.; Lombardi, F. Weldability and Monitoring of Resistance Spot Welding of Q&P and TRIP Steels. *Metals* **2016**, *6*, 270.
10. Wloka, J.; Laukant, H.; Glatzel, U.; Virtanen, S. Corrosion properties of laser beam joints of aluminium with zinc-coated steel. *Corros. Sci.* **2007**, *49*, 4243–4258. [CrossRef]

11. Almeida, E.; Morcillo, M. Lap-joint corrosion of automotive coated materials in chloride media. Part 2—Galvannealed steel. *Surf. Coat. Technol.* **2000**, *124*, 180–189. [CrossRef]
12. Tzeng, Y.F. Effects of process parameters on the corrosion rate of pulsed Nd:YAG laser-welded zinc-coated steel. *J. Mater. Proc. Technol.* **2002**, *124*, 1–7. [CrossRef]
13. Lukin, V.I.; Kovalchuk, V.G.; Kondrashov, E.K.; Malova, N.E.; Golev, E.V. Resistance spot welding of high-strength steels through new corrosion-resisting coatings. *Weld. Int.* **2010**, *24*, 963–968. [CrossRef]
14. Mei, L.; Yan, D.; Chen, G.; Xie, D.; Zhang, M.; Ge, X. Comparative study on CO_2 laser overlap welding and resistance spot welding for automotive body in white. *Mater. Des.* **2015**, *78*, 107–117. [CrossRef]
15. Mei, L.; Yi, J.; Yan, D.; Liu, J.; Chen, G. Comparative study on CO_2 laser overlap welding and resistance spot welding for galvanized steel. *Mater. Des.* **2012**, *40*, 433–442.
16. Banerjee, G.; Pal, T.K.; Bandyopadhyay, N.; Bhattacharjee, D. Effect of welding conditions on corrosion behaviour of spot welded coated steel sheets. *Corros. Eng. Sci. Technol.* **2011**, *46*, 64–69.
17. Davoodi, A.; Esfahani, Z.; Sarvghad, M. Microstructure and corrosion characterization of the interfacial region in dissimilar friction stir welded AA5083 to AA7023. *Corros. Sci.* **2016**, *107*, 133–144. [CrossRef]
18. Vincent Proton, V.; Alexis, J.; Andrieu, E.; Delfosse, J.; Lafont, M.C.; Blanc, B. Characterisation and understanding of the corrosion behaviour of the nugget in a 2050 aluminium alloy friction stir welding joint. *Corros. Sci.* **2013**, *73*, 130–142. [CrossRef]
19. Sabbaghzadeh, B.; Parvizi, R.; Davoodi, A.; Moayed, M.H. Corrosion evaluation of multi-pass welded nickel-aluminum bronze alloy in 3.5% sodium chloride solution: A restorative application of gas tungsten arc welding process. *Mater. Des.* **2014**, *58*, 346–356. [CrossRef]
20. Gharavi, F.; Matori, K.A.; Yunus, R.; Othman, N.K.; Fadaeifard, F. Corrosion behavior of Al6061 alloy weldment produced by friction stir welding process. *J. Mater. Res. Technol.* **2015**, *4*, 314–322. [CrossRef]
21. Huang, C.A.; Wang, T.H.; Han, W.C.; Lee, C.H. A study of the galvanic corrosion behavior of Inconel 718 after electron beam welding. *Mater. Chem. Phys.* **2007**, *104*, 293–300. [CrossRef]
22. Wu, W.; Hu, S.; Shen, J. Microstructure, mechanical properties and corrosion behavior of laser welded dissimilar joints between ferritic stainless steel and carbon steel. *Mater. Des.* **2015**, *65*, 855–861. [CrossRef]
23. Rossi, S.; Fedel, M.; Deflorian, F.; Vadillo, M.C. Localized electrochemical techniques: Theory and practical examples in corrosion studies. *C. R. Chim.* **2008**, *11*, 984–994. [CrossRef]
24. Deng, Y.; Peng, B.; Xu, G.; Pan, Q.; Ye, R.; Wang, Y.; Lu, L.; Yin, Z. Stress corrosion cracking of a high-strength friction-stir-welded joint of an Al-Zn-Mg-Zr alloy containing 0.25 wt. % Sc. *Corros. Sci.* **2015**, *100*, 57–72. [CrossRef]
25. Thomä, M.; Wagner, G.; Straß, B.; Wolter, B.; Benfer, S.; Fürbeth, W. Ultrasound enhanced friction stir welding of aluminum and steel: Process and properties of EN AW 6061/DC04-Joints. *Mater. Sci. Technol.* **2017**, in press.
26. Gharavi, F.; MAtori, K.; Yunus, R.; Othman, N.K.; Fadaeifard, F. Corrosion evaluation of friction stir welded lap joints of AA6061-T6 aluminum alloy. *Trans. Nonferr. Met. Soc. China* **2016**, *26*, 684–696. [CrossRef]
27. Liu, C.; Chen, D.L.; Bhole, S.; Cao, X.; Jahazi, M. Polishing-assisted galvanic corrosion in the dissimilar friction stir welded joint of AZ31 magnesium alloy to 2024 aluminum alloy. *Mater. Charact.* **2009**, *60*, 370–376. [CrossRef]
28. AWS D8.9M. *Test Methods for Evaluating the Resistance Spot Welding Behavior of Automotive Sheet Steel Materials*; American Welding Society (AWS): Miami, FL, USA, 2012.
29. ISO 9227:2017. *Corrosion Tests in Artificial Atmospheres—Salt Spray Tests*; International Organization for Standardization (ISO): Geneva, Switzerland, 2017.
30. Pouranvari, M.; Marashi, S.P.H. Critical review of automotive steels spot welding: Process, structure and properties. *Sci. Technol. Weld. Join.* **2013**, *18*, 361–403. [CrossRef]
31. Pouranvari, M.; Asgari, H.T.; Mosavizadch, S.M.; Marashi, P.H.; Goodarzi, M. Effect of weld nugget size on overload failure mode of resistance spot welds. *Sci. Technol. Weld. Join.* **2007**, *12*, 217–225. [CrossRef]
32. Huin, T.; Dancette, S.; Fabrègue, D.; Dupuy, T. Investigation of the failure of advanced high strength steels heterogeneous spot welds. *Metals* **2016**, *6*, 111. [CrossRef]
33. Liang, J.; Zhang, H.; Qiu, X.; Shi, Y. Characteristics of the resistance spot welding joints in dissimilar thickness dual-phase steels. *ISIJ Int.* **2015**, *55*, 2002–2007. [CrossRef]
34. Chao, Y.J. Failure modes of spot welds: Interfacial versus pullout. *Sci. Technol. Weld. Join.* **2013**, *8*, 133–137.